

SPHEROMAK COMPRESSION EXPERIMENTS AT GENERAL FUSION

**A. Froese, S. Howard, V. Suponitsky, J. Zimmermann, M. Reynolds, S. Barsky, J. McCone,
R. Ivanov, D. Parfeniuk, P. O'Shea, D. Richardson, M. Delage, M. Laberge**
General Fusion Inc., Burnaby, Canada

Abstract

In order to demonstrate the core physics of the magnetized target fusion process pursued by General Fusion, the company is experimenting with compressing spheromaks. The spheromaks are produced in a 30 cm diameter aluminum flux conserver, which is accelerated to an implosion speed of 2.5 km/s using 3 kg of high explosive. Better than 99% circular symmetry up to a 13:1 radial compression without rupture or buckling is achieved with this technique. Results from the liner compression development and from the spheromak plasma compression are presented.

1. Introduction

Magnetized Target Fusion (MTF) was first proposed in the 1970's as a low-cost approach to fusion that combines the advantages of magnetic confinement fusion and inertial confinement fusion by working in an intermediate regime of plasma density and confinement time. The U.S. Naval Research Laboratory did pioneering work on the LINUS program [1], which was unique among MTF schemes by employing a liquid metal liner to address the traditional fusion challenges of heat extraction, tritium breeding, and neutron flux on structural components [2, 3]. The liquid liner made the compression inherently repeatable, but at the time could not be accelerated to sufficiently high velocities to compress plasma within its thermal lifetime. General Fusion is pursuing an acoustically-driven MTF concept that makes use of modern servo controllers which precisely time piston impacts to create an acoustic wave in the liquid metal liner. This wave will compress the target plasma in less than 200 μ s, similar to the practically achievable plasma lifetimes in modern self-organized plasma devices.

In General Fusion's design (Figure 1), the deuterium-tritium fuel is supplied as a pair of magnetized plasma rings, known as spheromaks [4]. The spheromaks are delivered to an evacuated vortex inside a volume of liquid Pb-17Li eutectic metal (83 at% Pb, 17 at% Li) for the duration of an acoustically-driven spherical collapse. As the cavity volume decreases, the plasma density and temperature will grow to the point that the fuel will begin to fuse. Most of the fusion energy is liberated as neutron radiation that directly heats the liquid metal, which can then be pumped through a heat exchange system. Liquid Pb-17Li is ideal as a liner because it has a low melting point (507 K), low vapor pressure (10^{-4} Pa @ 700 K), breeds tritium, has a high density (9 g/cm³) to maximize the inertial dwell time of the compression, and has a good acoustic impedance match to steel (16 versus 44 MRayl), which is important for efficiently generating the acoustic pulse. The 100 MJ acoustic pulse is generated mechanically by hundreds of pneumatically-driven pistons striking the outer surface of the reactor sphere. The acoustic pulse propagates radially inwards, strengthened by geometric focusing from 10^3 to 10^4 MPa at the surface of the vortex.

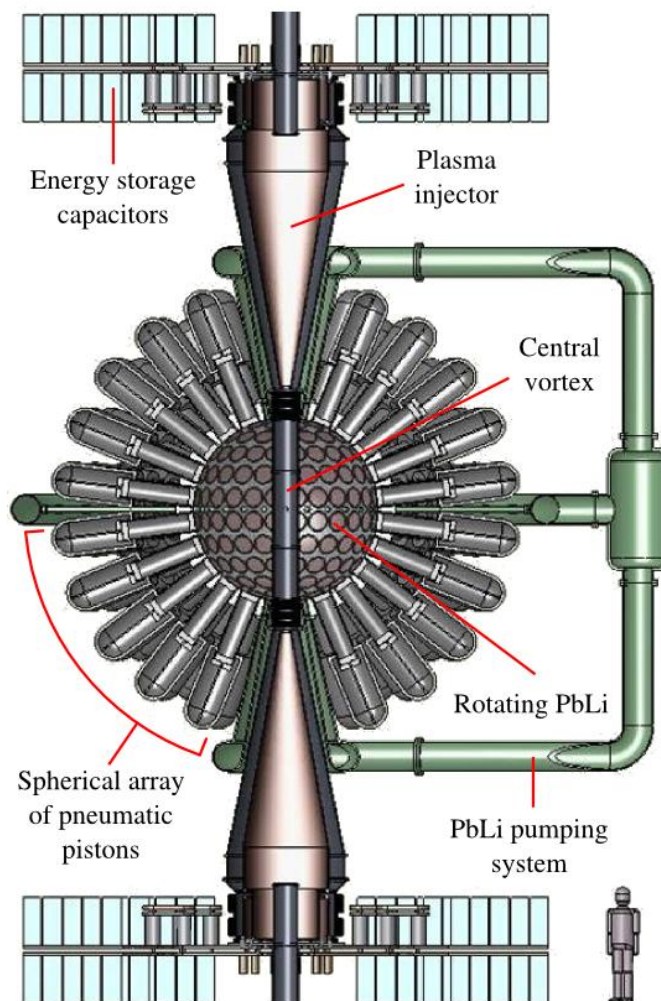


Figure 1: Schematic of envisioned commercial reactor.

General Fusion's design relies on the fundamental proposal that a magnetized plasma will heat adiabatically as the conducting chamber in which it is confined is compressed. The planned compression will reduce the cavity volume by at least three orders of magnitude, which is believed will raise the plasma density from 10^{17} ions/cm³ to 10^{20} ions/cm³, the temperature from 0.1 keV to 10 keV (for an adiabatic constant of 5/3), and the magnetic field strength from 6 T to 600 T. General Fusion's efforts are focused on testing the theory of plasma compression by forming a spheromak inside an aluminum chamber and compressing it using high explosives. To date, four such Plasma Compression Small (PCS) experiments have been performed, with three more scheduled in the next year.

This paper summarizes the General Fusion's activities during 2012 and 2013 surrounding the PCS experiments. Section 2 explains how a spheromak is generated. Section 3 lists the various diagnostics that are used to monitor the plasma behavior. Section 4 describes the techniques required to properly condition the device for use. Section 5 is an account of the development of the explosive driver. Section 6 explains how simulation results were used to improve plasma behavior by modifying the shape of the flux conserver. Section 7 describes the sustainment method for further improving plasma confinement. Finally, Section 8 contains a summary of the development timeline.

2. Spheromak Generation

The magnetized plasma for the PCS experiments is generated by a single-stage coaxial Marshall gun (Figure 2a) [5]. An initial poloidal magnetic flux of 20 mWb (Figure 2b) is generated by a coil of 100 turns wrapped around the central ferromagnetic tube and driven with 80 A of current. Deuterium gas is injected into the machine by 8 fast puff valves arranged around its base. A 3000- μ F capacitor bank charged to 20 kV is discharged through the gas to form a plasma and inject toroidal magnetic flux into the flux conserver (Figure 2c). Large induced currents on the surface of the flux conserver prevent magnetic field from escaping the enclosed volume, but can also melt the surface, so the flux conserver must be made of tungsten-coated aluminum wherever possible, which has low electrical resistance and is less vulnerable to heat damage than bare aluminum.

Once the Marshall gun ceases to inject toroidal flux, the magnetic fields in the plasma quickly self-organize to form a spheromak. In a spheromak, each magnetic field line spirals poloidally and toroidally. Most field lines do not retrace themselves, even after many turns around the torus, but can form so-called flux surfaces (Figure 2d). Heat flux is much smaller perpendicular to magnetic field lines rather than parallel to them. Therefore, if flux surfaces are nested concentrically, then the plasma is well insulated and good energy confinement is achieved. Unfortunately, many varieties of plasma instabilities exist that perturb these flux surfaces and reduce the confinement of the plasma.

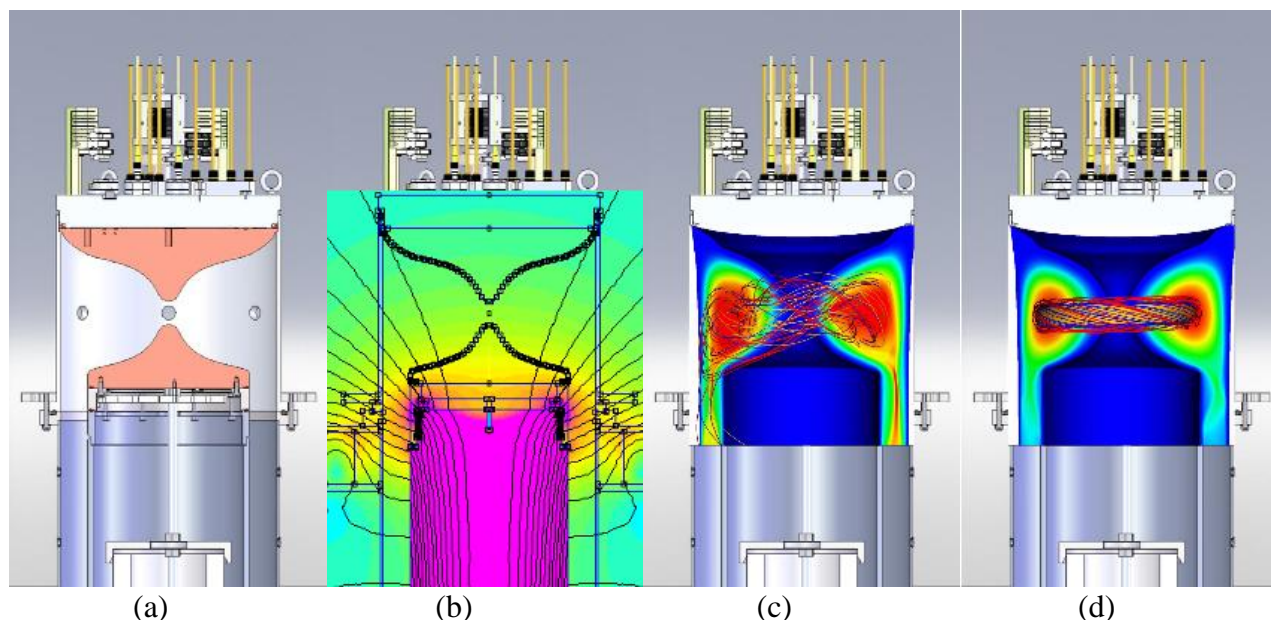


Figure 2: (a) Schematic of Marshall gun with a PCS2-type flux conserver. (b) Calculated poloidal magnetic field contours before discharge. (c) Simulated spheromak during formation before magnetic field lines have become self-organized. (d) Simulated flux surfaces after fully formed.

3. Diagnostics

Plasma diagnostic probes are arranged as tightly as possible all around the flux conserver. The magnetic field of the plasma is observed with 28 toroidal and poloidal magnetic pickup coils placed near the interior surface of the metal. Interferometers at 3 different radial positions record the line-averaged plasma density. Visible light emitted by the plasma is measured by an array of survey spectrometers with a sequence of exposure times that span the plasma compression, as well as by a set

of fiber-coupled photodiodes recording the time history of total visible emission at 3 positions. An ion Doppler spectrometer measures the time evolution of the ion temperature along a single line of sight.

The core electron temperature is measured by a single-point Thomson Scattering (TS) system once each discharge. The duration of the Thomson laser pulse is 10 ns. This sensitive diagnostic is only used during laboratory operation and is not possible during an actual high explosive compression in the field. Figure 3 shows an ensemble of electron temperature measurements taken in the plasma center. They are plotted as a function of time since spheromak formation, though each point is from a separate shot. The temperature is seen to increase with time because of Ohmic heating.

Plasma confinement can be calculated from a collection of diagnostic probes. The resistance of the plasma can be estimated from its temperature using the classical Spitzer resistivity relation [6]. The plasma current and Ohmic heating power are calculated from the edge magnetic field measurement. From the plasma density (heat capacity) measured by the interferometer and the rate of change of temperature one can calculate the rate of heat losses. For these sustained shots, the diffusion rate is $\chi = a^2/6\tau = 7 \text{ m}^2/\text{s}$ [4] for our energy confinement time ($\tau=60 \text{ }\mu\text{s}$) and plasma radius ($a=0.05 \text{ m}$). This is comparable to the Bohm diffusion rate of $\chi_{\text{Bohm}} = (1/16) T_e/B = 9 \text{ m}^2/\text{s}$ for our temperature ($T_e=290 \text{ eV}$) and magnetic field ($B=2 \text{ T}$). The Bohm diffusion formula [4, 6] is an empirical scaling law for the heat diffusion that was discovered early in fusion research. Bohm diffusion can be used to conservatively estimate power plant efficiency because it gives a lower bound for confinement compared to other possible scaling laws.

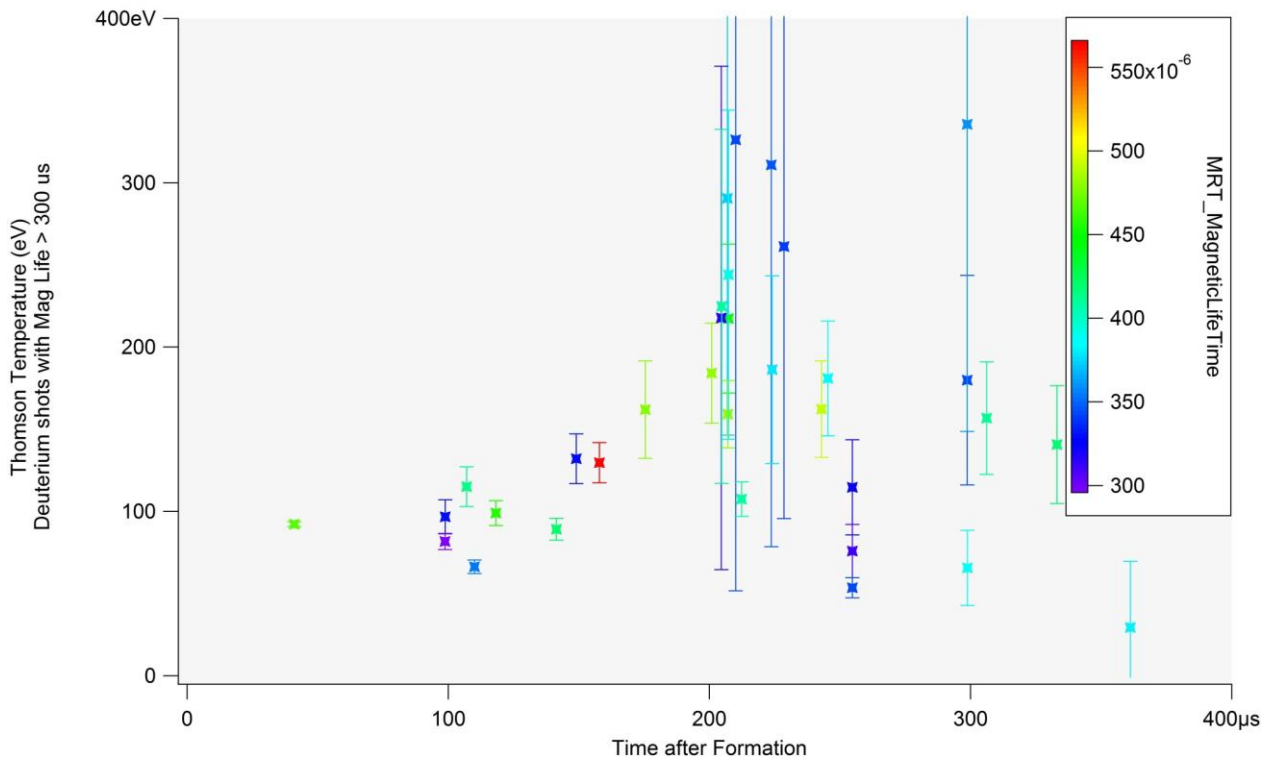


Figure 3: Electron temperatures as measured by Thomson scattering at different times after spheromak formation. The data shown are for deuterium shots with a magnetic lifetime greater than 300 μs.

4. Wall conditioning

Extreme care is required to reduce plasma contamination by material that may be emitted from the wall. Wall-sourced impurities can include trapped water, hydrocarbon residues, as well as the metallic components of the wall itself, and act to cool the plasma directly by radiation and charge exchange. Ions with bound electrons are the dominant source of radiative cooling due to the brightness of line radiation (photons from energy level transitions of bound electrons), and the effect is worst for high atomic number impurities that maintain bound electrons even into the range of $T_e > 1$ keV. Charge exchange cooling is dominantly due to a wall-recycling process of the main deuterium component of the plasma. A cold neutral deuterium atom from the wall can diffuse into the plasma across magnetic lines, then charge-exchange its one electron with a hot plasma ion, resulting in a cold ion and a hot neutral that promptly escapes the system. When the neutral returns to the wall, the process can repeat, making this a powerful cooling mechanism. Fresh titanium (Ti) on the wall can adsorb deuterium, making its release from the wall less likely. After about 5 deuterium shots, the Ti layer becomes saturated and a new layer must be deposited on top of the old one to maintain its efficacy.

A rigorous multi-step process is necessary to reduce the cooling effects of line radiation and charge exchange. Standard high-vacuum preparation of the system, followed by a 150 °C bake for 3 days is performed each time the machine is opened to air. After baking, about 300 discharges with helium are fired to clean the surfaces. Spectrometer measurements show that impurity concentrations steadily decrease during these shots. The lifetime and temperature of the plasma also slowly improve. Once good performance is achieved with helium shots, ~150 nm of Ti is evaporated onto the inside surfaces of the flux conserver by 3 heated Ti-balls. Finally, the gas is switched to deuterium and testing begins.

5. Explosive Driver

The focus of the plasma compression liner development at General Fusion has been on the design of a compression system for 30-cm diameter spheromaks. Explosives are used to drive the compression so as to do so in a directed and controlled manner while also allowing good diagnostic access to the plasma. The compression must reach completion in less than 100 μ s, faster than the rate at which the plasma decays. Therefore, the cylindrical liner is made of aluminum so as to have a very low mass. It is surrounded by 3 kg of RDX or PETN and accelerated to an implosion speed of 2.5 km/s.

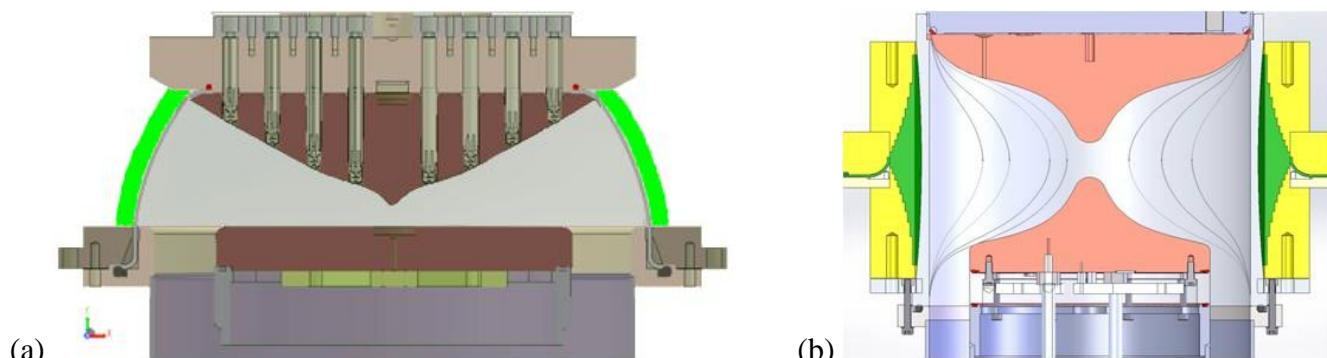


Figure 4: (a) Bowtie compression geometry – The vacuum region is shown in light grey and the copper flux conserver in dark red. Explosives are shown in green. Magnetic pickup coils (brown) in sets of 4 are inserted into the flux conserver from above. (b) Cone geometry with a pinching liner – The vacuum region is shown in light blue and the copper flux conserver in orange. Explosives are shown in green. Liner positions mid-flight are drawn as thin black lines.

The first Plasma Compression Small (PCS) shot was performed with the bowtie geometry shown in Figure 4a. The bowtie geometry used a liner that moved along a pseudo-spherical trajectory, sliding past the angled top and bottom walls so as to produce the maximum volumetric compression. Unfortunately, the sliding motion allowed explosive gases to move ahead of the liner and contaminate the plasma. The solution was to replace the sliding motion with a pinching motion, thereby preventing the passage of gases past the liner. This new compression liner design with conical flux conservers is shown in Figure 5.

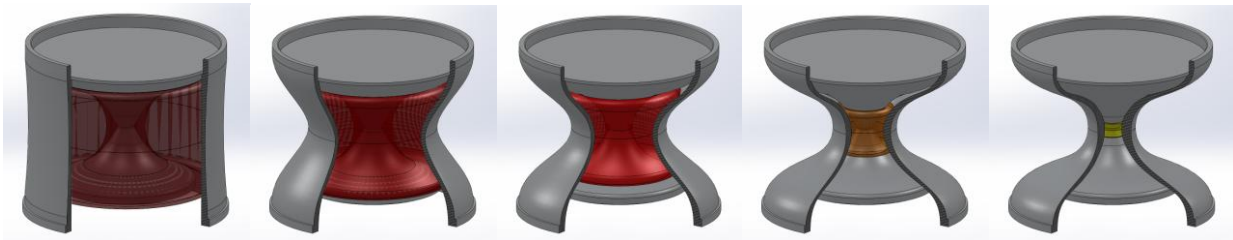


Figure 5: Sequential stages of the liner compression.

Theoretically, the pinching method should have eliminated the problem of explosive gas ingress, but issues involving circumferential tearing, ruptures, and wrinkling were still encountered. Figure 6 depicts these issues in high speed images of cylindrical liner implosions viewed axially. Figure 6a shows circumferential tearing near the outer edge of the implosion and wrinkling near the center of the implosion. Circumferential tearing is caused by tensile strains in the liner. Strain occurs in the transition zones between the moving and stationary portions of the liner. As center of the liner is squeezed inwards, it is pulled away from stationary edges of the liner and stretches the portion of the liner wall in between. The wrinkles are seeded by perturbations in the explosive gases and are exacerbated by a high liner-diameter-to-wall-thickness ratio. Typically these are caused by imperfections in the explosive lenses or the main explosive charge.

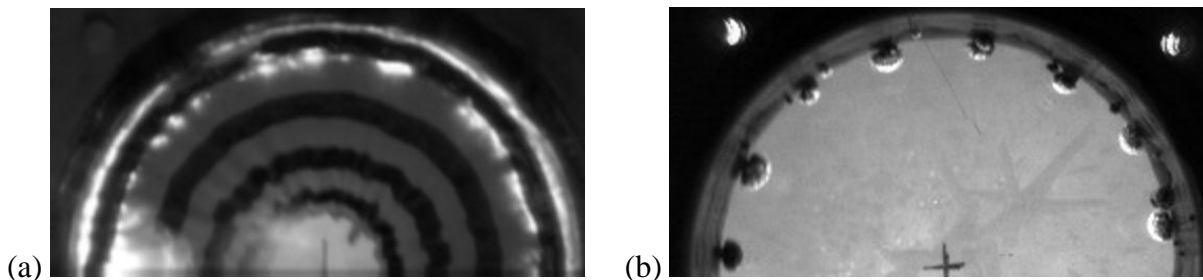


Figure 6: Issues with liner implosion shown in high-speed photographs: (a) Circumferential tearing and wrinkling (b) Rupturing through the liner.

An implosion with ruptures in the liner is shown in Figure 6b. The ruptures are periodic about the circumference of the implosion and the period matches the distribution of explosive lenses about the main charge. This indicates that the explosive lenses are not forming a uniform, circular detonation front in the main explosive charge and are instead forming periodic regions of high shock pressure that rupture the liner. To mitigate the circumferential tearing ductile 6061-O aluminum was chosen as the liner material and the walls at the liner's tensile regions were thickened. Computer modeling was used to determine the level of thickening that was required. The liner that had circumferential tearing in Figure 6a was first modeled using a radially symmetric two dimensional model of the imploding liner. As can be seen in Figure 7a, the model accurately predicts this tearing at the top and bottom of the liner

wall. For the subsequent model shown in Figure 7b the liner was thickened towards the edges of the wall and this model predicts that the tearing is eliminated.

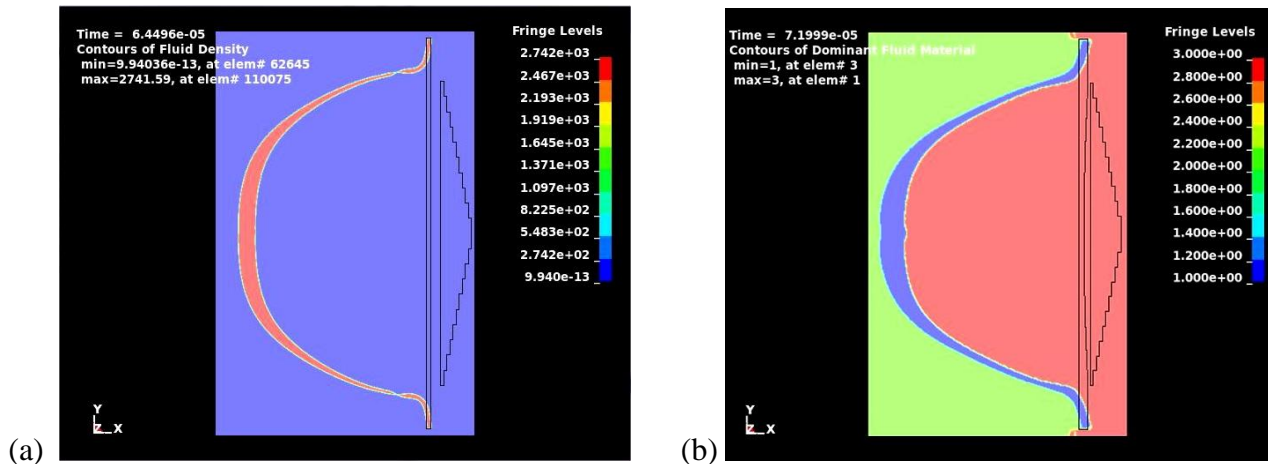


Figure 7: LS-Dyna simulation results in r-z cylindrical coordinates, axis left. The jagged triangular contour and two vertical black lines on the right indicate the starting position of the explosives and flyer plate, respectively. (a) Density plot showing circumferential tearing near the top and bottom of the liner wall. (b) Results for thicker liner showing good compression with empty space shown in green, the liner shown as blue, and explosive gases shown as pink.

To address the ruptures and wrinkling, the explosive lenses were improved and the wall thickness of the liner was increased. In the explosive lens optimization experiments shown in Figure 8, the explosive lens detonations are viewed directly with a high speed camera and brightness is interpreted as a measure of detonation pressure. To optimize the explosive lenses, their geometry was subtly changed to minimize the brightness variation on a circular chord at a diameter equivalent to the liner diameter. The optimized configuration shown in Figure 8d still contains regions with brightness variations; however it gives the most symmetric result at the diameter of the liner.

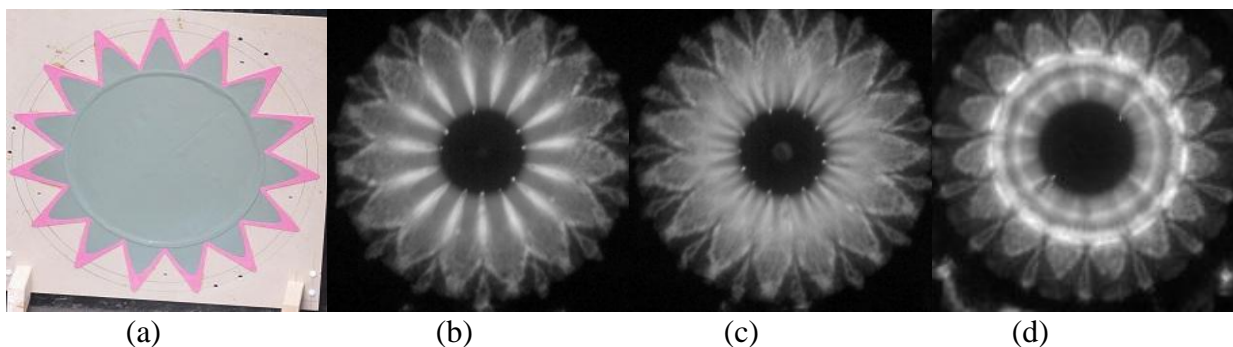


Figure 8: The explosive lens optimization. (a) The configuration of the explosive lenses used in this test. (b, c, d) High-speed photographs of the detonation showing the explosive lenses are progressively improving.

The sequence of high speed camera images shown in Figure 9 shows the results of the improvements of the liner implosion. Wrinkles, ruptures and circumferential tears have all been eliminated in this liner. The last frame in this sequence is at 13.7:1 compression and remains smooth and symmetric about the center.

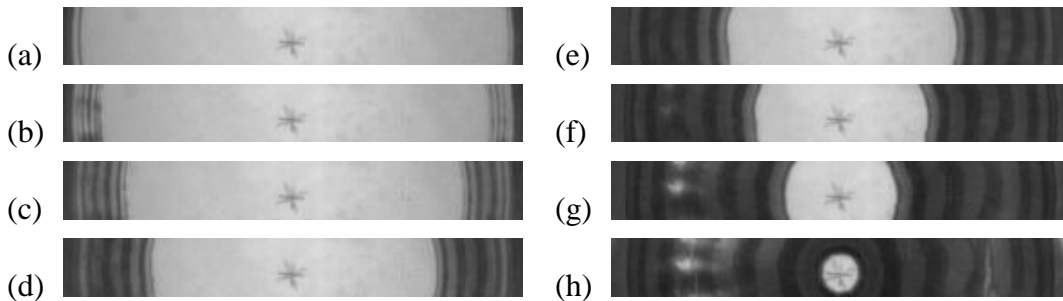


Figure 9: High-speed photographs of liner compression after wrinkles, ruptures and circumferential tears have been eliminated.

6. Tilt Stability

Some plasma instabilities that are unique to MTF plasmas are those that appear when the geometry of the flux conserver changes. Simulation results, backed up by experimental data from PCS2 and PCS3, showed that the cone geometry caused the spheromak to tilt and become non-axisymmetric partway through the compression.

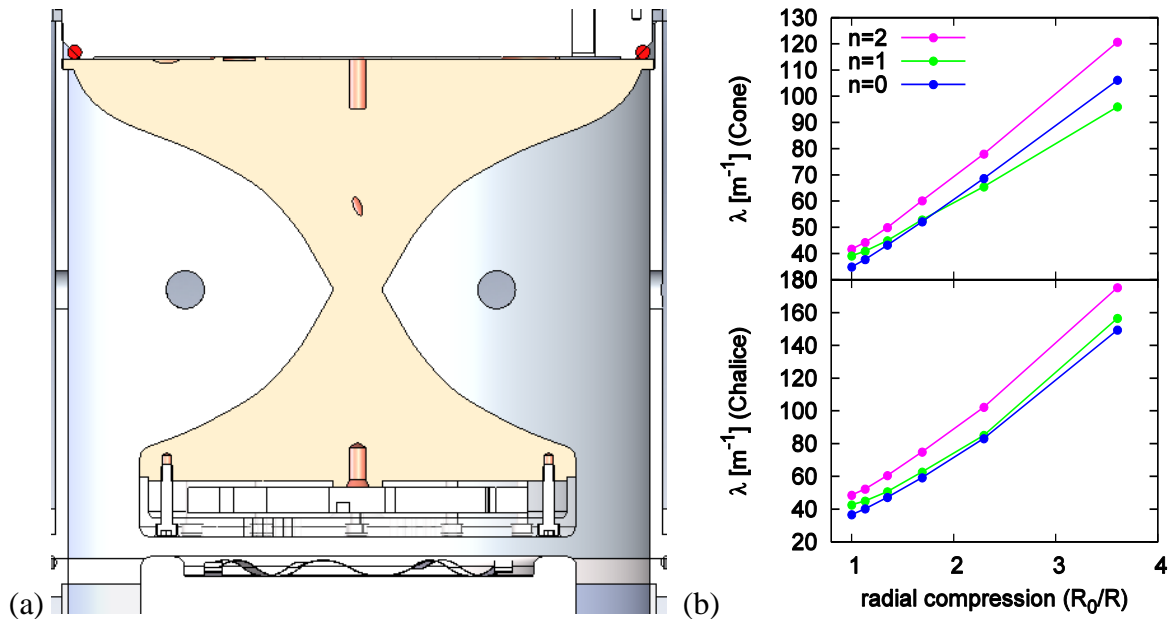


Figure 10: (a) Chalice geometry with good volumetric compression and low safety factor late in the compression. (b) Lambda eigenvalue for cone and chalice geometries at various radial compression ratios. The geometry is tilt-stable when the $n=0$ eigenvalue is smaller than the $n=1$ eigenvalue. [7]

A new chalice geometry for the inner electrode was developed to maintain tilt stability throughout the compression (Figure 10a). This was done by ensuring the safety factor q -profile of an axisymmetric Taylor-relaxed plasma was below unity for the entire range of geometries encountered during the compression. The plasma equilibrium was calculated with the Grad-Shafranov solver CORSICA, taking into account the flux present due to external coils. The design was also verified by calculating eigenvalues of the flux conserver using the M3D code [7] and verifying that the symmetric ($n=0$)

eigenvalue was always lower than the asymmetric ($n=1$) eigenvalue (Figure 10b). The same eigenvalue analysis showed that the gap between the electrodes in earlier experiments would result in tilt instability partway through the compression. Eigenvalue analysis does not answer the question of MHD stability of an actual history-dependent current distribution, of course. For insight into that question MHD simulation is required.

A multistage process was used to evaluate the stability of the spheromak during compression in each of the two flux conserver geometries: cone and chalice. All simulations were carried out using a version of the MHD simulation code Versatile Advection Code (VAC) [8] that has been modified for our

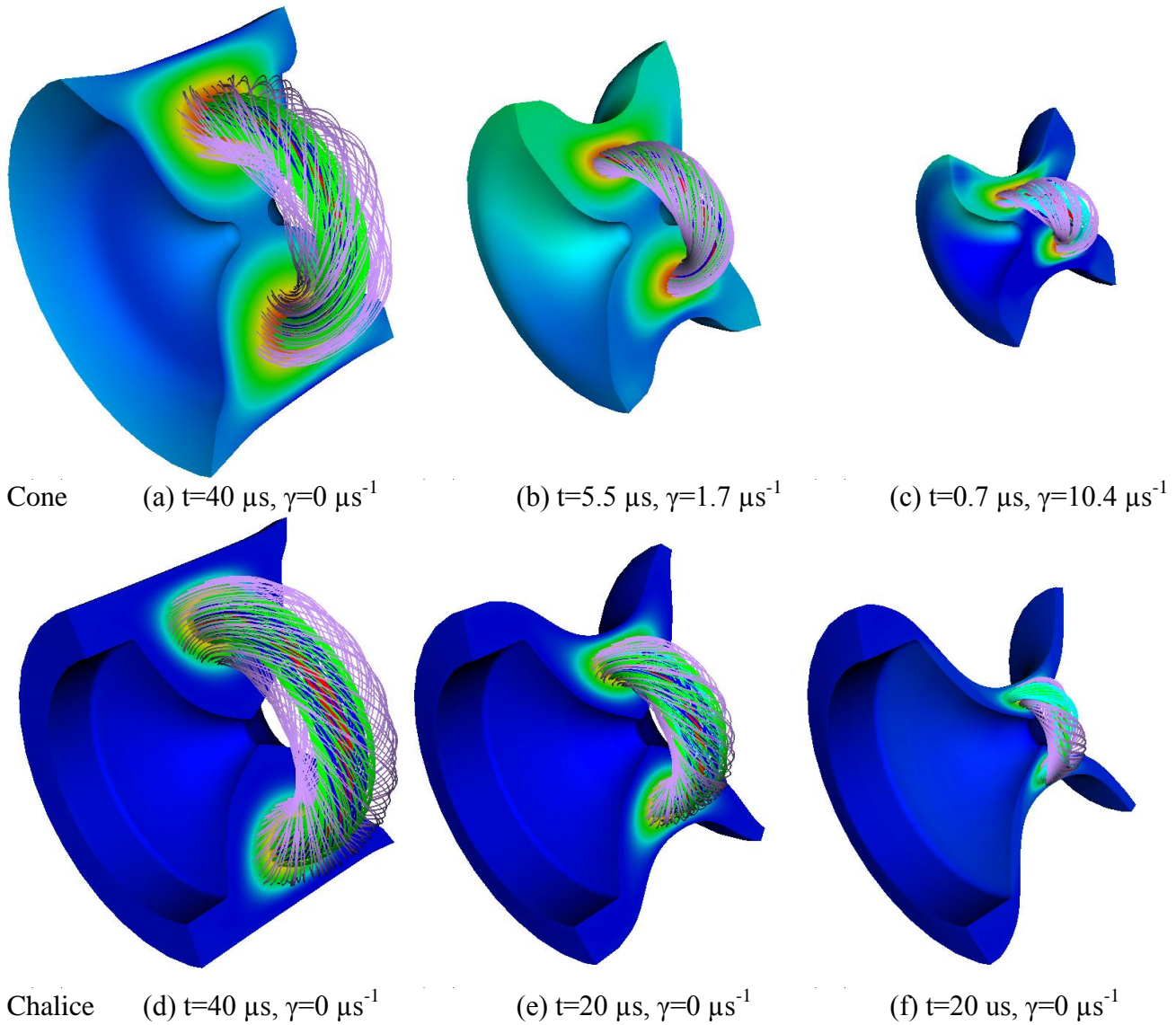


Figure 11: Growth rate of tilt instability for cone (a, b, c) and chalice (d, e, f) geometries at different compression stages: $R/R_0=1$ (a, d), $R/R_0=0.6$ (b, e), and $R/R_0=0.3$ (c, f). These simulations have a static flux conserver but are initialized using toroidally-perturbed 2d Grad-Shafranov equilibria that are generated assuming no flux loss occurs during compression. The rate of growth γ of the $n=1$ toroidal mode is evaluated at the time t shown.

purposes. The following procedure was used to prepare 3D simulations of the compression. (i) The geometry of the liner throughout compression was calculated by LS-Dyna software (proprietary). These results were closely benchmarked against dry compressions. Based on the liner geometry, computational meshes were constructed for flux conserver geometries at three different stages of the compression, when the radial compression ratios were $R(t)/R_0=1.0, 0.6$ and 0.3 . (ii) Axisymmetric plasma equilibria were calculated for each geometry using the Grad-Shafranov equation solver Corsica [9]. It was assumed that the flux conserver was perfectly conducting throughout the compression, i.e. no toroidal or poloidal flux was lost. (iii) The resulting equilibria were then used as initial conditions for the 3D VAC simulations in static, partially-compressed geometries. A small toroidal perturbation in density was added to seed any potential 3D instabilities in the plasma. If the partially-compressed spheromaks remained axisymmetric, then they were tilt-stable, but if they quickly fell apart, then they were susceptible to the tilt instability.

The results of the MHD simulations, which are shown in Fig. 11, corroborate the equilibrium calculations done by Corsica and M3D. The first row shows the spheromak in the cone geometries after it has had some time to evolve from its initial state. One can see that in the case of the uncompressed pot (Fig. 11a), the spheromak does not exhibit any instabilities and remains axisymmetric and well-confined for long times ($t=40 \mu\text{s}$). However, the situation is very different once the flux conserver becomes compressed. The spheromak tilts and does so faster as compression progresses (Fig. 11b, c). The rate at which the tilt instability grows is quantified by Fourier transforming the toroidal component of the magnetic field with respect to toroidal angle and calculating the spatial average of the $n=1$ mode amplitude. In the most compressed geometry the tilt mode amplitude grows exponentially with growth rate $\gamma=10.4 \mu\text{s}^{-1}$. The results of the chalice geometry are shown in the second row. The new geometry remains axisymmetric for long periods of time at all stages of compression. Our next step is to perform full 3D compression simulations with a moving mesh and compare the results with the present stability investigation. This work is in progress and will be reported elsewhere.



Figure 12: Photograph of PCS5 preparation with sustainment inductors in front of plasma injector.

7. Sustainment

A novel method for improving confinement was developed for the Sustained Spheromak Physics Experiment (SSPX) [10]. Typically, after the initial current pulse forms the spheromak, the current from the capacitor goes to zero. However, the plasma stability was found to improve considerably by sustaining the current at a reduced level after the initial pulse.

The sustainment method has been found equally effective in the General Fusion devices. The initial pulse current is about 700 kA for 20 μ s, which is now followed by a sustain current of 180 kA decaying with a L/R time constant of 2 ms. The inductors necessary to produce the sustainment pulse are shown front and centre in Figure 12. The magnetic field from a successful deuterium shot with sustain current is shown in Figure 13, labeled as the upcoming “PCS5 2014/04” shot. Oscillations in the magnetic probe signals are due to instabilities that reduce confinement. After an initial period with some turbulence, the plasma becomes very calm for 400 μ s until a final bout of turbulence develops at 500 μ s and terminates the discharge. With this technique, General Fusion can now generate a spheromak that has the potential to heat to the thermonuclear regime, as long as compression does not degrade the confinement.

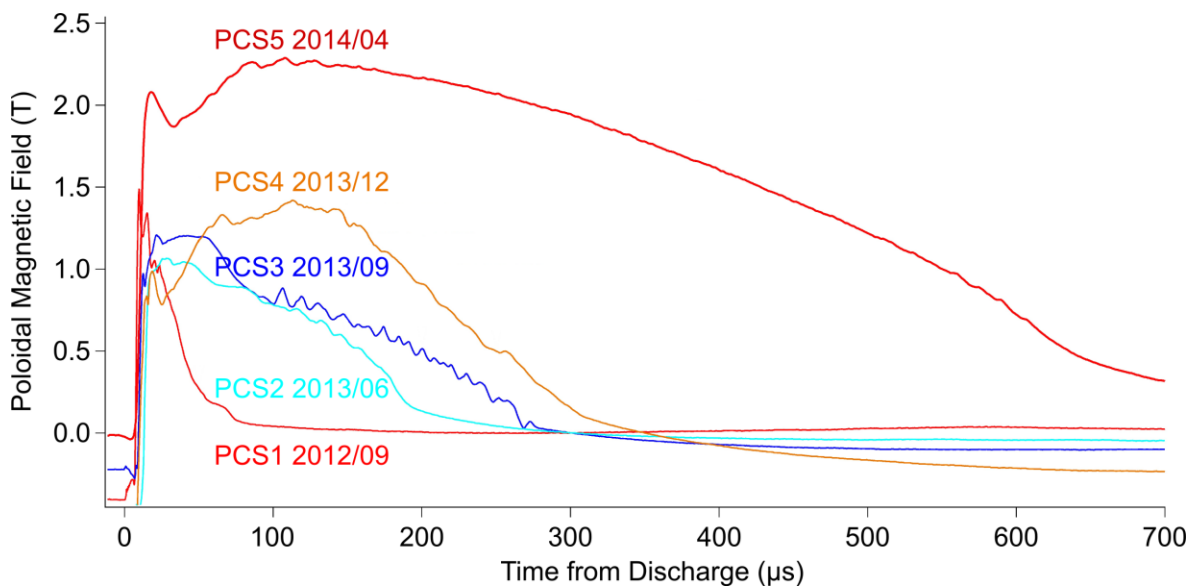


Figure 13: Poloidal magnetic field strength at one location on the wall versus elapsed time during historically successful deuterium shots immediately preceding a PCS shot.

8. Timeline Summary

To date, four Plasma Compression Small (PCS) experiments have been executed in a very short time frame.

- PCS1 was performed on 25th May 2012 using the bowtie geometry shown in Figure 4a. All diagnostics performed correctly and the data was stored successfully for post-analysis. In review, the design of this experiment was discovered to allow entry by explosive gases into the vacuum chamber, poisoning the plasma, and quenching it on a short time scale.
- PCS2 was conducted on the 8th June 2013 and employed a new pinch-style compression. This proved successful at isolating the explosives from the plasma by bending the liner instead of

fracturing it. Titanium gettering was used to reduce neutral recycling from the wall. The plasma lasted much longer than PCS1 and was partially compressed.

- PCS3 was conducted on September 29th 2013 and employed a thicker liner to produce much better compression symmetry. The results were marginally better than PCS2, suggesting compression symmetry and neutral recycling were not the dominant cause of confinement loss.
- PCS4 was conducted on the 14th December 2013 and utilized the tilt-stable chalice geometry. Magnetic measurements showed that tilt was eliminated and plasma confinement was improved.

Three more PCS experiments are scheduled over the course of the next year. Plasma performance is steadily increasing and we expect to improve upon previous tests by orders of magnitude. With the exception of the MAGO project [11, 12], this is the only family of MTF devices designed to be explosively-driven and the PCS experiments are the only ones to be publicly documented.

Acknowledgements

We would like to acknowledge the entire General Fusion engineering team for constructing all the experiments and keeping the equipment in proper running order.

9. References

- [1] R.L. Miller and R.A. Krakowski, "Assessment of the slowly-imploding liner (LINUS) fusion reactor concept", 4th ANS Topical Meeting on the Technology of Controlled Nuclear Fusion, 1980 October.
- [2] R. Siemon, et al., "Why Magnetized Target Fusion Offers A Low-Cost Development Path for Fusion Energy", Comments on Plasma Physics and Controlled Fusion, 1997.
- [3] R. Siemon et al., "The relevance of Magnetized Target Fusion (MTF) to practical energy production, a white paper for the Fusion Energy Sciences Advisory Committee", *Los Alamos National Labs*, 1999,
http://fusionenergy.lanl.gov/Documents/MTF/MTF_Appl._whitepaper_6-99.PDF
- [4] P.M. Bellan, *Spheromaks*, Imperial College Press, London, 2000, pp 210.
- [5] J. Marshall, "Performance of Hydromagnetic Plasma Gun", *Phys. Fluids*, Vol. 3, 1960, pp 134.
- [6] J.D. Huba, *NRL Plasma Formulary*, Office of Naval Research, Washington, D.C., 2009.
- [7] George Marklin, PSI Center, University of Washington, private communication
- [8] G. Tóth, "General Code for Modeling MHD flows on Parallel Computers: Versatile Advection Code", *Astrophysical Letters & Communications*, Vol. 34, No. 245, 1996, pp 471.
- [9] J.A. Crotinger, et al., "Corsica: A comprehensive simulation of toroidal magnetic-fusion devices", Report UCRL-ID-126284, Lawrence Livermore National Laboratory, 1997.
- [10] E.B. Hooper, et al. "Sustained Spheromak Physics Experiment (SSPX): design and physics results", *Plasma Phys. Control. Fusion*, Vol. 54, 2012, pp 26.
- [11] S.F. Garanin, et al. "Update on MAGO Progress", IEEE Megagauss Conference, 2006, pp 37.
- [12] I.R. Lindemuth, et al., "Target Plasma Formation for Magnetic Compression/Magnetized Target Fusion", *Phys. Rev. Lett.* Vol. 75, 1995, pp 1953.